

## **UWB-BASED GEOFENCING: A ONE-CLASS CLASSIFICATION APPROACH WITH FINGERPRINTING AND TRILATERATION**

*UDC ((711.5+004.775):004.021)*


**Sandra Đošić, Milica Jovanović,  
Milijana Veljković, Goran Lj. Đorđević**

University of Niš, Faculty of Electronic Engineering,  
Department of Electronics, Republic of Serbia


ORCID iDs: Sandra Đošić

 <https://orcid.org/0000-0002-1857-3603>


Milica Jovanović

 <https://orcid.org/0000-0002-5421-1343>

Milijana Veljković

 <https://orcid.org/0009-0006-3564-799X>

Goran Lj. Đorđević

 <https://orcid.org/0000-0003-3919-7835>

**Abstract.** *Ultra-wideband (UWB) technology has emerged as a powerful solution for indoor localization, offering high accuracy, low power consumption, and robust penetration through obstacles. Among its applications, geofencing enables the creation of virtual boundaries for monitoring and security purposes. This paper presents a novel one-class classification (OCC) approach for UWB-based geofencing, named the  $k$ -Nearest Neighbours with Residual Norm Threshold ( $k$ NN-RNT) algorithm. The proposed method utilizes fingerprinting and trilateration techniques, operating in two distinct phases: an offline phase for constructing a reference fingerprint database and an online phase for real-time classification of a mobile tag's location. The  $k$ NN-RNT algorithm determines geofence violations by analysing the distribution of nearest fingerprints and computing a residual norm to classify locations. A filtering mechanism enhances detection stability, mitigating noise and transient errors. Experimental validation in a controlled indoor environment demonstrates the effectiveness of the method, achieving over 99% accuracy within the geofenced area and significantly reducing classification errors in proximity zones. The proposed approach provides a reliable and efficient solution for real-time UWB-based geofencing applications.*

**Key words:** *Geofencing, ultra-wideband technology, one-class classification algorithm, fingerprinting, trilateration.*

---

Received April 09, 2025 / Accepted June 16, 2025

**Corresponding author:** Sandra Đošić

University of Niš, Faculty of Electronic Engineering, Department of Electronics, Aleksandra Medvedeva 4, 18000 Niš, Republic of Serbia

E-mail: [sandra.djosic@elfak.ni.ac.rs](mailto:sandra.djosic@elfak.ni.ac.rs)

## 1. INTRODUCTION

Ultra-wideband (UWB) is a wireless communication technology that utilizes a wide spectrum of frequencies to facilitate high-precision distance measurement and data transmission [1]. In recent years, UWB has gained significant attention due to its unique attributes, which make it particularly effective for radio-frequency-based indoor localization [2]. This technology offers both fine-range resolution for accurate distance measurements and high penetration capabilities, enabling signals to pass through various materials. Furthermore, UWB demonstrates adaptability to diverse environments while maintaining low power consumption, ensuring efficiency and sustainability. Importantly, its low-power emissions present minimal risks to human health and privacy, positioning UWB as a safe and versatile solution for a wide range of applications.

UWB technology excels in 2D and 3D positioning and tracking, particularly in environments where GPS signals are unreliable, such as indoor or underground settings. In industrial contexts, UWB enables precise tracking of equipment and materials, optimizing workflow and inventory management. In healthcare, it facilitates real-time monitoring of patients and medical assets, enhancing operational efficiency and safety. Furthermore, UWB supports advanced home automation systems by enabling accurate localization of individuals and objects, thus improving the responsiveness of smart devices. One of the key applications of UWB is geofencing, which establishes virtual boundaries within a physical space [3, 4]. The geofencing is critical for scenarios such as ensuring equipment remains within designated factory zones, alerting healthcare staff to patient movements beyond safe areas, or triggering automated actions in smart homes based on occupants' locations.

Geofencing, when treated as an indoor localization problem, can be effectively addressed using one-class classification (OCC), a machine learning technique designed for scenarios where only data from a single class is available [5, 6]. The OCC model is trained using offline UWB measurements collected within the designated area, capturing signal characteristics such as time-of-flight and received signal strength. These measurements define the reference class, enabling the model to recognize authorized locations and detect anomalies in real time. Unlike traditional multi-class classification, which distinguishes between predefined categories, OCC learns the characteristics of the geofenced area without prior knowledge of outliers [7, 8]. Deviations, such as a target leaving (or entering) the area, are treated as anomalies. This approach ensures reliable monitoring, allowing geofencing systems to detect and respond to irregularities with high accuracy, enhancing security and spatial integrity.

This paper proposes the k-Nearest Neighbours with Residual Norm Threshold (kNN-RNT) algorithm, a novel OCC method for UWB-based real-time tracking and geofencing. The kNN-RNT integrates fingerprinting and trilateration techniques to estimate the position of a mobile tag relative to a predefined geofencing area, using a system of three fixed anchors. The method operates in two phases: an offline phase, where a fingerprint database is constructed by scanning a 2D zone to train a single-class model, and an online phase, where the model evaluates new measurements to determine the tag's location. A filtering mechanism further refines the classification, enhancing detection reliability. Experimental results demonstrate the algorithm's effectiveness, achieving over 99% accuracy within the geofenced area and significantly reducing error rates in surrounding zones, from 34% at 5 *cm* to less than 1% at 20 *cm*.

The remainder of this paper is organized as follows. Section 2 reviews related studies on UWB-based indoor localization, focusing on geofencing and real-time tracking. Section 3

introduces the system model, followed by the proposed method in Section 4. Experimental results are discussed in Section 5, followed by conclusions in Section 6.

## 2. RELATED WORKS

Ultra-Wideband radio technology is widely recognized for its high temporal resolution and ability to resolve individual multipath components. These characteristics make UWB highly suitable for precise indoor distance measurements, making it a preferred choice for indoor localization research [9-11]. One of the most comprehensive survey papers on UWB indoor positioning is by Mazhar et al. [10], which provides an in-depth review of methods, algorithms, and implementations used in UWB-based positioning systems. The paper also presents a comparative analysis of UWB versus narrowband signals, demonstrating UWB's superior performance in complex indoor environments. Similarly, Campaña-Bastidas et al. [11] focus on the application of UWB for indoor positioning, particularly for elderly monitoring. Their study highlights the benefits of UWB's high precision and reliability in ensuring safety within indoor spaces.

Geofencing, which defines virtual boundaries within a physical space, depends on accurate localization techniques to determine whether an entity is inside or outside a designated area. Several recent studies have explored geofencing in indoor localization, as referenced in [12-17]. SIABR [16] takes a fingerprinting-based approach, constructing a location-specific fingerprint database and using bi-directional models to infer user positions with high precision. Fidora [17] investigates the use of channel state information (CSI) to create location-specific datasets for training machine learning classifiers, enabling accurate geofencing predictions. Additionally, [18] examines the integration of fingerprinting with UWB technology, leveraging UWB's fine-grained distance measurements to improve localization accuracy and reliability. Ardoin [19] explores the feasibility of applying Radio Frequency Fingerprinting (RFF) to UWB devices and assesses its generalizability across different environments. Furthermore, Malik et al. [20] investigate UWB-based positioning and ranging techniques, utilizing the channel impulse response (CIR) fingerprinting to enhance the localization accuracy.

One-Class Classification (OCC) has the potential to enhance geofencing applications by distinguishing between normal and anomalous location data. By training OCC models on data collected within the geofenced area, the system can effectively detect deviations, which may indicate unauthorized access or unusual activity, thereby improving the geofencing security and reliability. A comprehensive overview of OCC techniques is presented in [21], covering methods such as One-Class Support Vector Machine (OCSVM), Support Vector Data Descriptor (SVDD), One-Class Mini-Max Probability Machine, and Dual-Slope Mini-Max Probability Machine. Additionally, [22] investigates the use of OCC, particularly SVDD, for land cover classification from remotely sensed data. This study demonstrates how focusing on a single target class allows for efficient classification even with limited training data, highlighting the OCC's potential for geofencing applications.

### 3. SYSTEM MODEL

We consider a geofencing system deployed in a typical indoor environment with a complex layout, such as an office, classroom, or residential space, featuring multiple obstacles of varying sizes and shapes. Within this setting, the geofenced area is defined as a specific region, which can take a rectangular or any other shape depending on the application requirements. The localization infrastructure includes three anchor nodes situated at fixed and known positions, strategically placed to maximize coverage and accuracy within the geofenced area. These anchor nodes serve as reference points for the system. Additionally, there is a single mobile target node that is to be tracked as it moves within the indoor space. The target node periodically measures its distance to each anchor, and this data is used to determine whether it is inside or outside the predefined geofenced area. To ensure high accuracy and reliability of the distance measurements, it is required that a clear line-of-sight (LOS) condition is maintained between the target node and all three anchor nodes while the target is located within or near of the geofenced area. This assumption minimizes multipath effects and signal attenuation caused by obstructions, which are common in indoor environments, and is essential for achieving consistent geofencing performance using the UWB-based ranging.

The target and anchor nodes are implemented as UWB-enabled devices, which are capable of performing the Two-Way Ranging (TWR) procedure. The term "ranging" refers to the process of estimating the distance between two wireless devices measuring the signal time-of-flight (ToF) between two UWB-enabled devices and then multiplying this time measurement by the speed of light to obtain the distance. To facilitate accurate ToF measurements, commercial UWB transceivers are equipped with specialized circuitry that precisely timestamps the send and receive events at the physical level. Each UWB device uses its own local clock to create these timestamps. Consequently, the ranging process typically involves the exchange of three messages between the two UWB nodes, a method known as the TWR procedure.

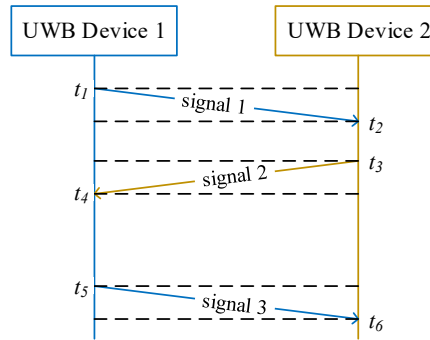


**Fig. 1** Two-Way Ranging procedure

The TWR procedure is presented in Fig. 1 and it works as follows:

1. UWB device 1 sends a message to the UWB device 2 (signal 1).
2. Upon receiving the message, UWB device 2 records the timestamp and immediately sends a response back to UWB device 1 (signal 2).

3. After receiving the response, UWB Device 1 sends another message to UWB Device 2 (Signal 3). This message contains all recorded timestamps from the previous signal exchanges.
4. By analysing the timestamps from these message exchanges, the system can accurately calculate the ToF according to Eq.1.

$$T_{tof} = \frac{[(t_4 - t_1) - (t_3 - t_2)] + [(t_6 - t_3) - (t_5 - t_4)]}{4} \quad (1)$$

The distance obtained through the TWR procedure represents the length of the shortest signal path between the two devices, ideally corresponding to their true physical separation. However, the accuracy of this measurement can be influenced by several factors, including multipath propagation, signal interference, clock synchronization errors, and hardware imperfections. In non-line-of-sight (NLOS) conditions, obstacles may cause signal reflections, leading to overestimated distances due to elongated signal paths. Despite these challenges, commercial UWB transceivers, such as those based on the IEEE 802.15.4a/z standard, typically achieve distance measurement accuracy of  $\pm 10$  cm under favourable conditions, with some high-precision implementations reducing errors to as low as a few centimetres in optimal line-of-sight scenarios, [23].

#### 4. PROPOSED ZONE DETECTION METHOD

The proposed zone detection method is implemented using a two-phase approach, consisting of an offline phase and an online phase.

##### 4.1. Offline phase

The offline phase involves conducting a detailed site survey to build two distinct fingerprint databases. The first dataset, referred to as the Interior Fingerprint Database (IFD), is created by systematically moving the tag across the entire geofenced area, ensuring a full coverage without any gaps. This database is later used during the online phase to detect whether the tag is inside the designated area. IFD and BFD are illustrated in Fig. 2. The second dataset, called the Boundary Fingerprint Database (BFD), is collected by moving the tag precisely along the perimeter of the geofenced area. This database plays a crucial role in training the system, as will be explained in a later section.

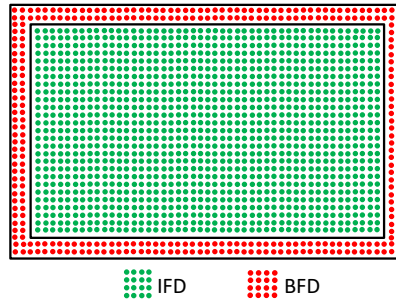


**Fig. 2** Interior (IFD) and Boundary (BFD) Fingerprint Database

We assume that the target node autonomously captures fingerprints through periodic ranging rounds. The frequency of these ranging rounds is a configurable system parameter, typically ranging from 10 to 50 rounds per second. In each ranging round, the target node executes the TWR procedure with each anchor node individually, recording the resulting range estimates as a *raw* fingerprint. Each raw fingerprint is represented as a vector,  $\mathbf{f} = (d_1, d_2, d_3)$ , where  $d_i$  denotes the TWR-measured distance between the target node and the  $i$ -th anchor. Since each point within the geofenced area corresponds to a unique combination of three distances to the anchor nodes, raw fingerprints inherently encode the tag's location.

The collected raw fingerprints are used to construct two types of fingerprint databases: plane and 2D. In the plane databases (IFD\_P and BFD\_P), fingerprints are stored in their original form, preserving the raw distance measurements to three anchor nodes. In contrast, the 2D databases (IFD\_2D and BFD\_2D) are created by mapping these distance measurements to 2D spatial coordinates,  $\mathbf{f} = (x, y)$ , using a trilateration procedure based on the known positions of the anchors. The trilateration is implemented via the least squares method to minimize positional estimation errors. Both database types are supported by the online detection method, allowing flexibility in geofencing scenarios. The method operates independently of the chosen representation, utilizing the appropriate fingerprint format for an accurate classification.

#### 4.2. Online phase

During the online phase, the system's primary task is to determine whether the tag is inside or outside the geofenced area based on real-time distance measurements and the IFD database. The overall procedure is as follows. In the online phase, the tag periodically generates distance vectors that represent its current position. If IFD\_2D database is used, each generated distance vector is transformed into 2D representation using trilateration procedure. To assess the tag's presence within the designated area, the system first employs an OCC algorithm. The output of this algorithm is a numerical value correlated with the tag's distance from the geofenced area. By comparing this value against a predefined threshold, the system produces a binary indication, signalling whether the tag is inside or outside the area. To mitigate the effects of noise and anomalies, a sequence of binary indications is processed through a filtering mechanism. The output of this filter provides the final, reliable indication of the tag's presence within the geofenced area. Next, we provide a more detailed description of the three key components of the zone detection method: the OCC algorithm, threshold determination, and the filtering mechanism.

For the zone detection, we employ our custom OCC algorithm, k-Nearest Neighbours with Residual Norm Threshold, which evaluates the uniformity of fingerprint distribution in proximity of the tag's current position. The algorithm is illustrated in Fig. 3, where cross marks represent three distinct tag positions: A (inside the geofenced area), B (on the perimeter), and C (outside the area). Given an online distance vector, the algorithm first identifies the  $k$  nearest fingerprints within the IFD database using Euclidean distance as the metric for similarity. Each fingerprint is represented as a vector originating from the tag's position. These  $k$  vectors are then summed, forming a residual vector (red arrows in Fig. 3). The magnitude of the residual vector is referred to as the residual norm. When the tag is inside the geofenced area, fingerprints from IFD are expected to be uniformly distributed around it, resulting in a small residual norm. When the tag is near the perimeter, most IFD

fingerprints will be concentrated on one side, leading to a moderate residual norm. If the tag is outside the geofenced area, all nearby fingerprints will be located in similar directions relative to the tag's position, producing a large residual norm. The farther the tag moves away from the geofenced area, the higher the residual norm becomes.

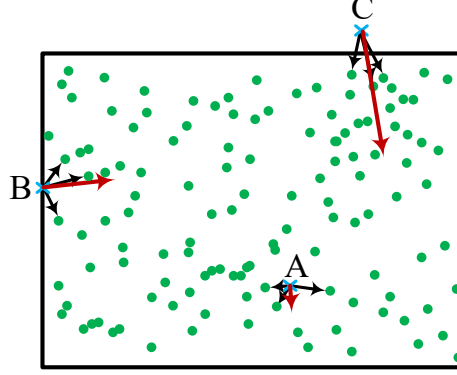


**Fig. 3** Illustration of kNN-RNT algorithm for  $k=3$

Let formalize this procedure. The current tag position is represented by the distance vector  $\mathbf{x} = (x_1, x_2, \dots, x_n)$ , while a fingerprint from IFD is denoted as  $\mathbf{f} = (f_1, f_2, \dots, f_n)$ . In the specific case of plane and 2D zone detection problems, where  $n = 3$  and  $n = 2$ , respectively, but we maintain an arbitrary  $n$  to highlight the generality of the method. Let,  $N = \{\mathbf{f}_i | i = 1, \dots, k\}$  be the set of  $k$  fingerprints in IFD nearest to the distance vector  $\mathbf{x}$ . The residual vector  $\mathbf{r} = (r_1, r_2, \dots, r_n)$  is then computed as:

$$r = \sum_{i=1}^k (x - f_i) \quad (2)$$

The norm of the residual vector is given by:

$$\rho = \sqrt{\sum_{i=1}^n r_i^2} \quad (3)$$

Once the residual norm  $\rho$  is computed for a given distance vector, the tag's presence within the geofenced area is determined by comparing  $\rho$  to a predefined threshold  $\tau$ . Specifically, if  $\rho < \tau$ , the tag is considered to be inside the area; otherwise, it is classified as outside.

The choice of the threshold value  $\tau$  is critical for ensuring the reliability of the detection method. If  $\tau$  is set too high, the system may generate frequent false positives, incorrectly classifying the tag as inside the zone when it is actually outside. Conversely, if  $\tau$  is too low, false negatives will occur, failing to detect the tag's presence within the geofenced area. The optimal  $\tau$  value depends on the density and distribution of fingerprints in the IFD database and cannot be selected independently of it. To determine an appropriate threshold, we utilize the BFD database, which consists of fingerprints collected along the perimeter of the geofenced area. At the perimeter, the tag's "inside/outside" status is ambiguous, meaning the probability of obtaining a residual norm above or below the threshold should be equal. To find such a threshold, we apply the kNN-RNT algorithm to each fingerprint in the BFD database and record the resulting residual norm values. These values are then sorted in

ascending order, and the median value is chosen as  $\tau$ . This approach ensures that half of the BFD fingerprints are classified as "inside the zone" and the other half as "outside," balancing the classification at the boundary.

To mitigate the impact of noisy distance measurements, the method incorporates a filtering mechanism based on a shift-register-like data structure. This structure maintains the  $L$  most recent binary indications, where a value of 1 signifies that the tag is inside the zone, and 0 indicates that it is outside. The final decision regarding the tag's presence is determined by a hysteresis-based approach:

- The system declares the tag inside the zone once the number of 1s in the register exceeds a predefined threshold  $T_1$ .
- Conversely, the system switches the tag's status to outside the zone only when the count of 1s drops below a lower threshold  $T_2$ , where  $T_2 < T_1$ .

This dual-threshold strategy prevents rapid fluctuations in the detection output due to the transient noise, ensuring a more stable and reliable classification.

## 5. IMPLEMENTATION AND EVALUATION

The experimental evaluation was conducted in a typical office environment using a geofencing system with Ultra-Wideband technology. The testbed consists of four UWB nodes: three fixed anchors and one target node. The anchor nodes were mounted 1.50 m above the floor and strategically arranged in an equilateral triangle with side lengths of 4.10 m to ensure optimal signal coverage within the geofenced area. The target node was attached to a movable tripod, also positioned 1.50 m above the floor, allowing controlled movement across various positions during the experiments. The system operates with a ranging interval of 20 measurements per second, configured via onboard firmware settings. The ranging measurements were wirelessly transmitted in real time to a laptop running a location server, where the zone detection algorithm was implemented. The laptop was equipped with custom software, written in Python, to process distance measurements, classify geofencing events, and log detection results for further analysis.

We use the Murata Type 2AB UWB Evaluation Kits for our nodes [24]. This kit integrates a Qorvo QM33120W UWB transceiver, a fully integrated impulse radio UWB wireless transceiver built for precise distance measurement [23], along with a Nordic nRF52840 Bluetooth Low Energy SoC and UWB patch antennas, all on a single PCB. The power source for all nodes consists of rechargeable lithium-ion batteries, ensuring stable voltage supply throughout the experiments.

The fingerprint databases for the zone detection method are constructed by systematically scanning the interior and perimeter of the geofencing area using the tag. The IFD databases (IFD\_P and IFD\_2D) contain a total of 4200 fingerprints, while the BFD databases (BFD\_P and BFD\_2D) comprise 1200 fingerprints. The kNN-RNT OCC algorithm is configured with  $k = 9$ , while the threshold parameter  $\tau$  is experimentally determined using the BFD databases, as outlined in the previous section. Since the threshold value depends on the type of fingerprint database, it is  $\tau = 0.48$  for the IFD\_P database and  $\tau = 0.66$  for the IFD\_2D database. The filtering mechanism utilizes a shift register of length  $L = 12$ , with upper and lower thresholds set to  $T_1 = 12$ , and  $T_2 = 4$ , respectively.

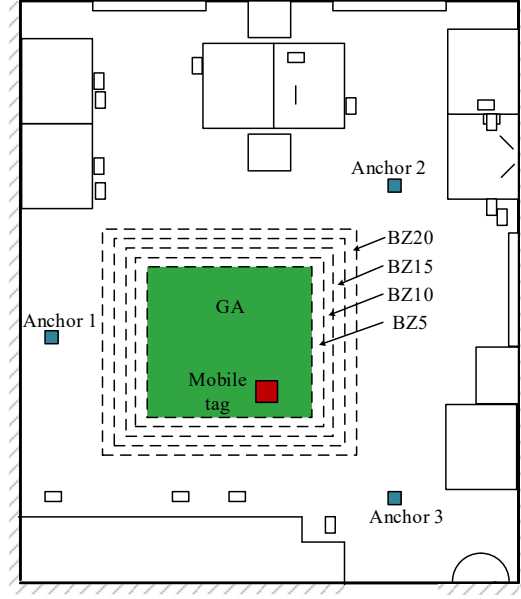


**Fig. 4** Experimental setup for zone detection method

The operation of our evaluation testbed is characterized by two timing parameters: latency and response time. Latency is defined as the time elapsed from the start of a ranging round at the target node to the completion of the classification task by the location server for the corresponding online fingerprint. The testbed provides a latency of  $24ms$  or  $26ms$ , depending on whether a plane or 2D fingerprint database is used, respectively. This latency comprises: *a)* the duration of the ranging round ( $20ms$ ), *b)* the time required to transmit distance measurements to the location server ( $2ms$ ), and *c)* the classification time, which is  $2ms$  for plane fingerprints and  $4ms$  for 2D fingerprints. The increased classification time for the 2D fingerprint database is due to an additional trilateration step, which maps the three measured distances to 2D spatial coordinates. The system response time is defined as the interval between the occurrence of an event, such as the target node crossing a geofencing boundary, and the moment the location server signals the event. This time is influenced by the duration of the ranging interval and the parameters of a shift-register-based filtering mechanism. In the adopted system configuration, the response time ranges from  $50ms$  to  $400ms$ , depending on the current state of the shift-register data structure. This delay is acceptable for most monitoring applications.

We conducted two sets of experiments to evaluate the accuracy and effectiveness of the proposed zone detection method. First, we assessed the method's ability to accurately determine whether the tag is inside or outside the geofencing area. Next, we examined its effectiveness in detecting tag entry and exit events.

### 5.1. Zone detection accuracy

In this set of experiments, the tag was moved along predefined paths. The system's "In/Out" responses were recorded and subsequently processed to evaluate the accuracy of zone detection.

Two metrics were utilized to assess the zone detection accuracy: In-Zone detection rate and Out-Zone detection rate represent the percentage of instances where the target node is identified as being within and outside the geofencing area, respectively. In the first experiment (denoted as GA), the tag followed a random path within the geofencing area. Since the tag never left the area, the expected In-Zone detection rate is 100%. In the second experiment (denoted as EZ), the tag moved along the perimeter of the geofenced area, where the expected In-Zone and Out-Zone detection rates are both 50%. For the next four experiments, the tag moved along surrounding belts of the geofencing area at a fixed distance from the perimeter. These experiments are labelled as BZ $x$ , where  $x \in \{5, 10, 15, 20\}$  denotes the distance in *cm* of the tag from the perimeter. Ideally, the Out-Zone detection rate for these experiments should be 100%.

The Fig. 5 illustrates the fingerprints collected during these experiments. Each point represents a 2D location derived by applying the trilateration procedure to a raw distance fingerprint vector captured by the tag. Green points correspond to the IFD database, created during the offline scanning of the geofencing area. The remaining points, distributed around the area, were recorded during online testing as the tag was moved along predefined paths surrounding the area. The clear separation between differently coloured points suggests the potential for precise In-Zone/Out-Zone classification.

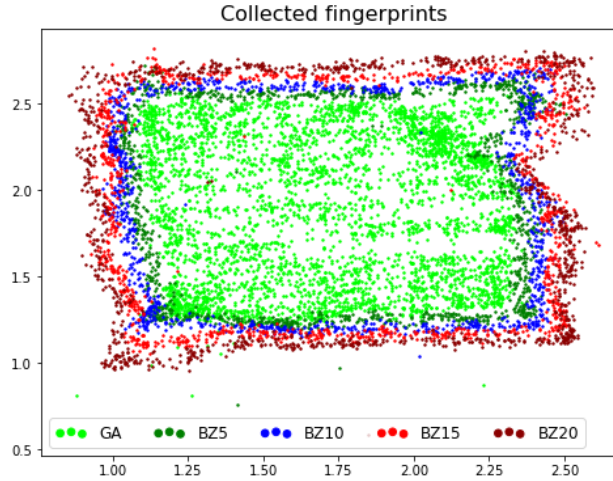


**Fig. 5** Collected fingerprints in GA and at a fixed distance from the perimeter

The zone detection rate results, for both plane and 2D databases, are summarised in Table 1. For the case when the tag moves within the geofencing area (GA) the method shows almost perfect zone detection accuracy of more than 99%. The very low Out-Zone rate of less than 1% indicates that there are minimal false negatives, where the tag presence inside the geofencing area are incorrectly identified as being outside. This high level of accuracy is crucial for applications that rely on precise geofencing, ensuring that the target node's location is accurately tracked and monitored within the designated area. The near-perfect 50/50% split between In-

and Out-Zone rates in the EZ experiment is expected, as the threshold  $\tau$  is determined using tag movements along the same path (i.e., the perimeter of the area) during the offline phase.

**Table 1** Zone detection rate results for plane and 2D fingerprint databases

		Plane fingerprint database	2D fingerprint database
GA	In [%]	<b>99.92</b>	<b>99.83</b>
	Out [%]	0.08	0.17
EZ	In [%]	50.12	50.02
	Out [%]	49.88	49.98
BZ5	In [%]	34.93	33.65
	Out [%]	<b>65.07</b>	<b>66.35</b>
BZ10	In [%]	19.89	12.38
	Out [%]	<b>80.11</b>	<b>87.62</b>
BZ15	In [%]	7.82	2.41
	Out [%]	<b>92.18</b>	<b>97.59</b>
BZ20	In [%]	5.31	0.66
	Out [%]	<b>94.69</b>	<b>99.34</b>

The zone detection rates for the BZx experiments indicate that the method is less confident when the tag is outside the geofencing area. This is an expected result, as the kNN-RNT algorithm is trained exclusively on fingerprints collected within the geofencing area, making it more sensitive and accurate when detecting the tag inside the area than when it is outside. As can be observed, the Out-Zone detection rate rises while the In-Zone detection rate falls as the tag moves farther from the boundary, reflecting its proximity to the geofencing area. With the plane fingerprint database, the Out-Zone detection rate rises from 65% at 5 *cm* from the boundary to 95% at 20 *cm*. The accuracy is higher with the 2D fingerprint database, providing an improvement of approximately 5% over the plane database. However, it is important to note that the use of the 2D database is computationally more demanding, as it requires performing the trilateration procedure for each sample.

In order to further validate the effectiveness of our kNN-RNT algorithm, we conducted a comparative analysis with three widely used OCC algorithms: One-Class Support Vector Machine (One-Class SVM), Mahalanobis Distances, and Isolation Forest, presented in Table 2. These algorithms are commonly employed for anomaly detection and spatial boundary tracking in geofencing applications. For all algorithms, we used the same dataset to ensure consistency in evaluation. Furthermore, to provide a fair comparison, we fine-tuned the parameters for each method, optimizing them to achieve their best possible performance. This ensures that our evaluation highlights the true capabilities of each approach under identical conditions.

**Table 2** Accuracy comparison of the kNN-RNT algorithm with three standard one-class classification methods

		2D fingerprint database	
		Algorithm	Hits [%]
GA	kNN-RNT		<b>99.83</b>
	One-Class SVM		99.64
	Mahalanobis Distances		99.64
	Isolation Forest		99.40
BZ5	kNN-RNT		<b>66.35</b>
	One-Class SVM		66.06
	Mahalanobis Distances		58.77
	Isolation Forest		58.03
BZ15	kNN-RNT		<b>97.59</b>
	One-Class SVM		91.30
	Mahalanobis Distances		95.01
	Isolation Forest		91.21

The results presented in Table 2 demonstrate that kNN-RNT consistently outperforms all baseline methods, achieving the highest hit rate across all test cases. As can be observed in the BZ5 scenario, both Mahalanobis Distance and Isolation Forest exhibit a significantly lower detection accuracy compared to One-Class SVM and kNN-RNT. However, while One-Class SVM performs competitively when the target node is located just outside the geofencing area, it consistently underperforms relative to kNN-RNT in other scenarios, further highlighting the robustness and superiority of our proposed method.

## 5.2. Real-time tracking results

In the second experiment, we aimed to emulate an application scenario for the proposed zone detection method, where the system identifies and signals a tag's entry into and exit from the geofencing area. Signalling is facilitated by a speaker that emits a brief tone whenever the tag enters or exits the area, with distinct frequencies assigned to the "enter" and "exit" tones. For this experiment, the tag is moved along paths perpendicular to the geofencing area, beginning approximately 30 *cm* outside its boundary. When the system emits the "entry" tone, the tag's current position is recorded as the entry point, and it continues moving toward a stop point located about 30 *cm* within the geofencing area. The tag is then returned along the same path to the starting point, and its position at the time of the "exit" tone is marked as the exit point. This procedure is repeated multiple times across different paths around the geofencing area.

The results of this experiment are illustrated in Fig. 6, showing recorded entry points (red dots) and exit points (blue dots) for 42 entry-exit paths. The accuracy of entry-exit detection varies along the area boundary due to multipath effects and interference, which impact UWB distance measurements. These effects are particularly pronounced in complex indoor environments, such as the space where the experiment was conducted. However, the observed variations remain within the expected UWB ranging accuracy of  $\pm 10$  *cm*. Note that all recorded entry and exit points are located outside the geofencing area. This is because, in this experiment, we used the same threshold parameter  $\tau$  as in the previous experiment, where it was optimized to minimize the Out-Zone detection rate for a tag moving within the geofencing area. As a result, the system prioritizes reliable detection of

the tag entering the area over detecting its exit. Practically, this means that the "entry" tone is always triggered just before the tag enters the geofencing area but never when it is already inside. Furthermore, the entry points remain relatively close to the area's boundary, with an average distance of 4.4 *cm* and a maximum of 8.5 *cm*. Exit points are consistently farther from the boundary than entry points, averaging 7.8 *cm* with a maximum distance of 11.5 *cm*.

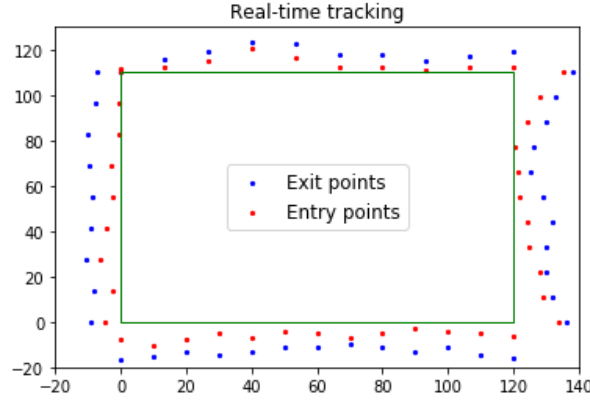


**Fig. 6** Entry (red dots) and exit points (blue dots) obtained in real-time tracking experiment

The results of the tracking experiment suggest that reducing the threshold parameter  $\tau$  could balance entry-exit detection accuracies. The expected effect would be shifting both entry and exit points closer to the geofencing boundary. Another source of entry-exit detection inaccuracy is the delay introduced by the filtering mechanism, which adds a latency of up to 8 samples when transitioning between in-zone and out-zone states, and vice versa. This delay, when multiplied by the tag's speed, translates into the spatial separation between entry and exit points along the same path. Reducing the length of the shift register could minimize this entry-exit discrepancy, but it may also increase variations in the detected distances from the area's boundary. However, in this paper, we do not further explore potential tracking optimizations related to the threshold parameter  $\tau$  or shift-register length.

## 6. CONCLUSIONS

This paper introduces the kNN-RNT algorithm, a novel OCC-based approach for real-time UWB geofencing. By utilizing fingerprinting and trilateration, the method effectively distinguishes between authorized and unauthorized locations using a residual norm thresholding mechanism. The two-phase operation ensures a robust geofence enforcement, with an offline phase constructing a reference fingerprint database and an online phase performing the real-time classification. Experimental results validate the high accuracy and reliability of the proposed approach, achieving over 99% detection accuracy within the geofenced zone. Furthermore, the method significantly reduces misclassification rates in transition areas by employing an adaptive thresholding strategy and a filtering mechanism.

The results showed a significant decrease in accuracy error, from 34% for the belt zone at 5 cm to less than 1% for the belt zone at 20 cm. The findings demonstrate the potential of kNN-RNT for applications in security, industrial automation, healthcare, and smart environments, offering a scalable and efficient geofencing solution for indoor localization systems.

Building on these promising results, future work will address practical deployment challenges. Although the proposed kNN-RNT algorithm demonstrates high accuracy in geofenced zone detection, its performance may be impacted by environmental factors such as multipath propagation, signal interference, and non-line-of-sight conditions, which can introduce variations in ranging precision. To enhance robustness under such conditions, we plan to explore dynamic geofencing techniques, in which adaptive models update fingerprints in response to environmental changes.

**Acknowledgement:** *This work has been supported by the Ministry of Science, Technological Development and Innovation of the Republic of Serbia [grant number 451-03-137/2025-03/200102].*

#### REFERENCES

- [1] Y. Rahayu, T. A. Rahman, R. Ngah, P. S. Hall, "Ultra wideband technology and its applications," *2008 5th IFIP International Conference on Wireless and Optical Communications Networks (WOCN'08)*, Surabaya, Indonesia, pp. 1-5, May 2009, doi: 10.1109/WOCN.2008.4542537
- [2] C. T. Li, J. C. Cheng, K. Chen, "Top 10 technologies for indoor positioning on construction sites," *Automation in Construction*, vol. 118, 103309, 2020, doi: 10.1016/j.autcon.2020.103309
- [3] D. S. Jachowski, R. Slotow, J. J. Millsbaugh, "Good virtual fences make good neighbors: opportunities for conservation," *Animal Conservation*, vol. 17 no. 3, pp. 187-196, 2014, doi: 10.1111/acv.12082
- [4] W. Zhuo, K. H. Chiu, J. Chen, J. Tan, E. Sumpena, S. H. G. Chan, C. H. Lee, "Semi-supervised learning with network embedding on ambient rf signals for geofencing services," *arXiv preprint*, 2025. [Online]. Available: <https://arxiv.org/abs/2210.07889>, doi: 10.48550/arXiv.2210.07889
- [5] Y. Yoo, J. Suh, J. Paek, S. Bahk, "Secure region detection using Wi-Fi CSI and one-class classification," *IEEE Access*, vol. 9, pp. 65906-65913, 2021, doi: 10.1109/ACCESS.2021.3076176
- [6] K. Fu, C. Gong, Y. Qiao, J. Yang, I. Guy, "One-class SVM assisted accurate tracking," *2012 Sixth International Conference on Distributed Smart Cameras (ICDSC)*, pp. 1-6, October 2012, doi: 10.1117/1.JEI.22.2.023002
- [7] C. Bellinger, S. Sharma, N. Japkowicz, "One-class versus binary classification: Which and when?," *2012 11th international conference on machine learning and applications*, vol. 2, pp. 102-106, December 2012, doi: 10.1109/ICMLA.2012.212
- [8] S. S. Khan, M. G. Madden, "One-class classification: taxonomy of study and review of techniques," *The Knowledge Engineering Review*, vol. 29 no. 3, pp. 345-374, 2014, doi: 10.1017/S026988891300043X
- [9] A. Alarifi, A. Al-Salman, M. Alsaleh, A. Alnafessah, S. Al-Hadhrani, M. Al-Ammar, H. Al-Khalifa, "Ultra wideband indoor positioning technologies: Analysis and recent advances," *Sensors*, vol. 16 no. 5, pp. 707, May 2016, doi: 10.3390/s16050707
- [10] F. Mazhar, M. G. Khan, B. Sällberg, "Precise indoor positioning using UWB: A review of methods, algorithms and implementations," *Wireless Pers. Commun.*, vol. 97 no. 3, pp. 4467-4491, Dec. 2017, doi: 10.1007/s11277-017-4734-x
- [11] S. Campaña-Bastidas, M. Espinilla-Estévez, J. Medina-Quero, "Review of Ultra Wide Band (UWB) for Indoor Positioning With Application to the elderly," *Hawaii International Conference on System Sciences*, pp. 1-10, January 2022, doi: 10.24251/HICSS.2022.269
- [12] M. T. Hoang, B. Yuen, X. Dong, T. Lu, R. Westendorp, K. Reddy, "Recurrent neural networks for accurate rssi indoor localization," *IEEE Internet Things J.*, vol. 6 no. 6, pp. 10 639-10 651, 2019, doi: 10.1109/JIOT.2019.2940368
- [13] L. Li, X. Guo, N. Ansari, "Smartloc: Smart wireless indoor localization empowered by machine learning," *IEEE Transactions on Industrial Electronics*, vol. 67 no. 8, pp. 6883-6893, Aug. 2020, doi: 10.1109/TIE.2019.2931261

- [14] R. Wang, H. Luo, Q. Wang, Z. Li, F. Zhao, J. Huang, "A spatial-temporal positioning algorithm using residual network and lstm," *IEEE Transactions on Instrumentation and Measurement*, vol. 69 no. 11, pp. 9251-9261, Nov. 2020, doi: 10.1109/TIM.2020.2998645
- [15] M. Zhou, Y. Li, M. J. Tahir, X. Geng, Y. Wang, W. He, "Integrated statistical test of signal distributions and access point contributions for wi-fi indoor localization," *IEEE Transactions on Vehicular Technology*, vol. 70 no. 5, pp. 5057-5070, May 2021, doi: 10.1109/TVT.2021.3076269
- [16] S. Fan, Y. Wu, C. Han, X. Wang, "Siabr: A structured intra-attention bidirectional recurrent deep learning method for ultra-accurate terahertz indoor localization," *IEEE Journal on Selected Areas in Communications*, vol. 39 no. 7, pp. 2226-2240, July 2021, doi: 10.1109/JSAC.2021.3078491
- [17] X. Chen, H. Li, C. Zhou, X. Liu, D. Wu, G. Dudek, "Fidora: Robust wifi-based indoor localization via unsupervised domain adaptation," *IEEE Internet of Things Journal*, vol. 9 no. 12, pp. 9872-9888, June, 2022, doi: 10.1109/JIOT.2022.3163391
- [18] S. Djosic, I. Stojanovic, M. Jovanovic, G. Lj. Djordjevic, "Multi-Algorithm UWB-based Localization Method for Mixed LOS/NLOS Environments," *Computer Communications*, vol. 181, pp. 365-373, 2022, doi: 10.1016/j.comcom.2021.10.031
- [19] T. Ardoin, N. Pauli, B. Groß, M. Kholghi, K. Reaz, G. Wunder "Tracking UWB Devices Through Radio Frequency Fingerprinting Is Possible," arXiv preprint, 2025. [Online]. Available: <https://arxiv.org/abs/2501.04401>, doi: 10.48550/arXiv.2501.04401
- [20] W. Q. Malik, B. Allen, "Wireless Sensor Positioning with Ultrawideband Fingerprinting," *The Second European Conference on Antennas and Propagation, EuCAP 2007*, Edinburgh, pp. 1-5, 2007, doi: 10.1049/ic.2007.0891
- [21] P. Perera, O. Poojan, M. P. Vishal, "One-class classification: A survey," arXiv preprint, 2021. [Online]. Available: <https://arxiv.org/abs/2101.03064>, doi: 10.48550/arXiv.2101.03064
- [22] C. Sanchez-Hernandez, S. B. Doreen, M. F. Giles, "One-class classification for mapping a specific land-cover class: SVDD classification of fenland," *IEEE Transactions on Geoscience and Remote Sensing*, vol. 45 no. 4, pp. 1061-1073, 2007, doi: 10.1109/TGRS.2006.890414
- [23] QM33120W, Fully Integrated Impulse Radio Ultra-Wideband (UWB) Wireless Transceiver. [Online]. Available: <https://www.qorvo.com/products/p/QM33120W>
- [24] Murata Type 2AB UWB Evaluation Kit. [Online]. Available: <https://www.murata.com/en-eu/products/connectivitymodule/ultra-wide-band/qorvo>